Thermomechanical Modeling of Orthogonal Cutting Including the Effect of Stick-Slide Regions on the Rake Face

E. Ozlu [1], E. Budak[1*], A. Molinari[2]
[1] Sabanci University, Faculty of Engineering and Natural Sciences, Orhanli, Tuzla 34956, Istanbul, Turkey,
[2] Laboratoire de Physique et Mécanique des Matériaux, UMR CNRS 7554, Université Paul Verlaine-Metz, Ile du Saulcy, 57045 Metz, France
* ebudak@sabanciuniv.edu

Abstract
An orthogonal cutting model including the primary and secondary shear zones is presented in this study. The primary shear zone is modeled by a thermomechanical model where the rake contact is represented by two regions of respectively sticking and sliding friction. The model is compared with experimental results in terms of shear stress, shear angle, and cutting force predictions. Overall a good agreement is observed.

1 INTRODUCTION

Modeling of orthogonal cutting has been one of the major problems for machining researchers for decades. Understanding the fundamental mechanics and dynamics of the orthogonal cutting process would result in solution of major problems in machining such as parameter selection, accurate predictions of forces, stresses, and temperature distributions. One of the first successful mathematical attempts for modeling of the mechanics of orthogonal cutting was made by Merchant [1]. Merchant [1] studied the formation of continuous chip by assuming that the chip is formed by shearing along a shear plane whose inclination was obtained from the minimum energy principle. Although his model has several important assumptions, it is still widely used to understand the basics of the cutting process. Later, many models were proposed [2-7] on the modeling of the orthogonal cutting process. After some deceleration in the research on cutting process mechanics due to the developments in CNC and CAD/CAM technologies, the process research regained some momentum in recent years. Many predictive models have been proposed by means of analytical, semi-analytical or completely numerical methods up to now. Semi-analytical models, where some of the parameters are identified from the cutting tests, usually yield high prediction accuracy, however they may not always provide insight about the process [8-10]. In addition, the cutting tests can be time consuming depending on the number of variables and their ranges. Numerical methods such as FEM [11-14] could provide much more detailed information about the process, such as temperature and pressure distribution, however they can be very time consuming. On the other hand, some analytical models may provide sufficient insight about the process. They can be categorized as the slip-line models [15-19], and thin and thick shear zone models [20-23].

It can be deduced from the previous studies that there are several accurate models for the primary shear zone. There are also several studies where the friction in machining is investigated [24-30]. However, there are still issues in modeling the rake contact zone which involves the friction between the tool and the workpiece due to the complicated nature of the chip-tool contact. In a recent study Ozlu and Budak [31] proposed an orthogonal cutting model that integrates the primary and secondary deformation zones' effects on the cutting process. In modeling of the primary shear zone the approach proposed by Dudzinski and Molinari [21] is used. They used a thermomechanical constitutive relationship which is transformed to a Johnson-Cook type material model in this study. The shear plane is modeled having a constant thickness. In their later model, Dudzinski and Molinari [21] modeled the friction on the rake face as a temperature dependent variable by considering the sliding contact conditions which is valid for high cutting speeds. In general, the material exiting from the primary shear zone enters the rake contact with a high normal pressure that creates a sticking friction region, i.e. plastic con-

tact, between the tool and the material. After a short distance, the contact state changes to sliding, i.e. elastic, due to the decreasing normal pressure which can be represented by Coulomb friction. Ozlu and Budak [31] considered this by modeling the rake face contact using dual zones.

In this study, an orthogonal cutting model is presented for the prediction of cutting forces. The model uses thermomechanical model for the primary zone and considers dual contact zone for the rake contact. The minimum energy approach is used for the shear angle prediction and the material model constants are calibrated directly from the cutting tests. The friction and material constants can be obtained from orthogonal cutting tests. Orthogonal tube cutting tests are conducted for the calibration. After calibration, the model can be used for different machining operations using the same tool and workpiece material. The outputs of the proposed model are the shear angle, shear stress in the shear plane, cutting forces, the stress distributions on the rake face, sliding friction coefficient, and the length of the sticking and sliding zones. Although the model is still under development, the final aim of the model is to develop a cutting process model which needs minimum amount of calibration tests.

The paper is organized as follows. The proposed mathematical formulation is presented in the next section. In section 3 the results obtained from the experimental results are presented and discussed.

2 PROCESS MODEL

In this section, the model for the orthogonal cutting process is presented together with the identification of the coefficient of friction between the tool and the workpiece materials. Firstly, the basic formulations regarding the primary and secondary shear zones are given, although the detailed derivation can be found in [31]. Then the tube cutting test setup is presented from where the coefficient of friction is identified. Finally different solution procedures are introduced in order to obtain the shear stress, cutting forces, stress distributions on the rake face and the length of the contact zones.

2.1 Modeling of the Primary and Secondary Shear Zones

The proposed model in this study includes the modeling of the primary and secondary shear zones in the orthogonal cutting process. The primary shear zone model is adapted from Dudzinski and Molinari [21] and the contact at the rake face is modeled by dual zone approach. Although the detailed mathematical model can be found at [21] and [22], it is presented here briefly. It should be mentioned here that the calculation of the shear angle is also included in this study which is one step ahead from the aforementioned study [31]. The main assumption in modeling the primary shear zone is that the shear plane has a thickness of h, and no plastic deformation occurs before and after the shear plane up to the sticking region at the rake face. The material behavior is represented with the Johnson-Cook constitutive model as follows:

$$\tau = \frac{1}{\sqrt{3}}\left[A + B\left(\frac{\gamma}{\sqrt{3}}\right)^{n}\right]\left[1 + \ln\left(\frac{\dot{\gamma}}{\dot{\gamma}_0}\right)^{m}\right]\left[1 - \left(\overline{T}\right)^{v}\right] \quad (1)$$

where γ is the shear strain, $\dot{\gamma}$ is the shear strain rate, $\dot{\gamma}_0$ is the reference shear strain rate, A, B, n, m, and v are material constants, and $\overline{T} = (T-T_r)/(T_m-T_r)$ where T is the absolute temperature, T_r is the reference temperature, T_m is the melting temperature. The material entering the primary shear zone sustains a shear stress of τ_0. When it leaves the primary shear zone the shear stress has evolved to the value τ_1 which is different from τ_0 when inertia effects are important. Assuming a constant thickness of the shear zone and a uniform pressure distribution, τ_0 can be iteratively calculated as proposed by [22]. Also from the equations of motion for a steady state solution and continuous type chip the shear stress at the exit of the shear plane is calculated as follows:

$$\tau_1 = \rho\left(V \sin\phi\right)^2 \gamma_1 + \tau_0 \quad (2)$$

where V is the cutting speed, ϕ is the shear angle and γ_1 is the strain due to the plastic deformation at the shear plane.

On the other hand, contact between the material and the workpiece at the rake face is modeled by a dual zone approach. This contact is divided into the sticking and sliding friction regions which was originally proposed by Zorev [3]. In the first region, the contact condition is plastic due to the high normal pressure exerted on the tool, whereas in the second region the contact is elastic which can be represented by sliding friction. Zorev [3], and later others [32-34], proposed shear and normal stress distribution on the rake face as shown in Figure 1.a.

However it is well known and also proved by friction tests [35] that the Coulomb friction coefficient cannot exceed 1.0 between metallic materials unless some kind of oxide formation or chemical reaction occurs [26,36]. Therefore, as shown by split tool cutting tests and mathematical analyses [18,28,35,37-39] the distributions of the shear and normal stresses on the rake face are considered to be as shown in Figure 1.b. which is used for the model in this study. In order to model the normal pressure on the rake face mathematically, the following distribution is selected [31]:

$$P(x) = P_0\left(1 - \frac{x}{\ell_c}\right)^{\zeta} \tag{3}$$

where ℓ_c is the contact length (see Figure 2), x is the distance on the rake face from the tool tip, and ζ is the exponential constant which represents the distribution of the pressure, and is selected as 3 in the current study.

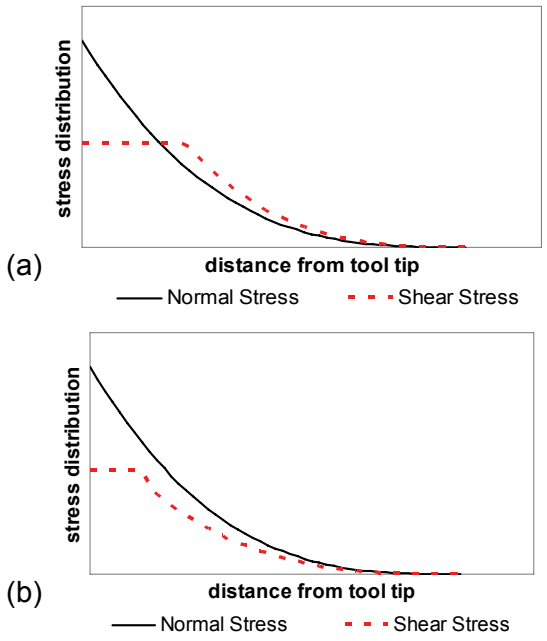

Figure 1: Stress distributions on the rake face by two different approaches, where the sliding friction coefficient is (a) higher, and (b) smaller than 1.

It can be observed from Figure 1.b, that the shear stress on the rake face is equal to the shear yield stress of the material (τ_1) along the sticking region with length ℓ_p. In addition, the shear stress in the sliding region is equal to the product of sliding friction coefficient (μ) and the normal stress (P), according to the Coulomb friction law. The shear stress reduces to zero at the end of the contact zone. Therefore, the mathematical representation of the shear stress distribution on the rake face can be defined as follows:

$$\begin{aligned} \tau &= \tau_1 && x \le \ell_p \\ \tau &= \mu P && \ell_p \le x \le \ell_c \end{aligned} \tag{4}$$

Moreover the shear stress distribution along the sliding friction region can be defined as follows:

$$\tau(x) = \tau_1\left(1 - \frac{x - \ell_p}{\ell_e}\right)^{\zeta} \qquad \ell_p \le x \le \ell_c \tag{5}$$

where ℓ_e is the length of the sliding region (see Figure2).

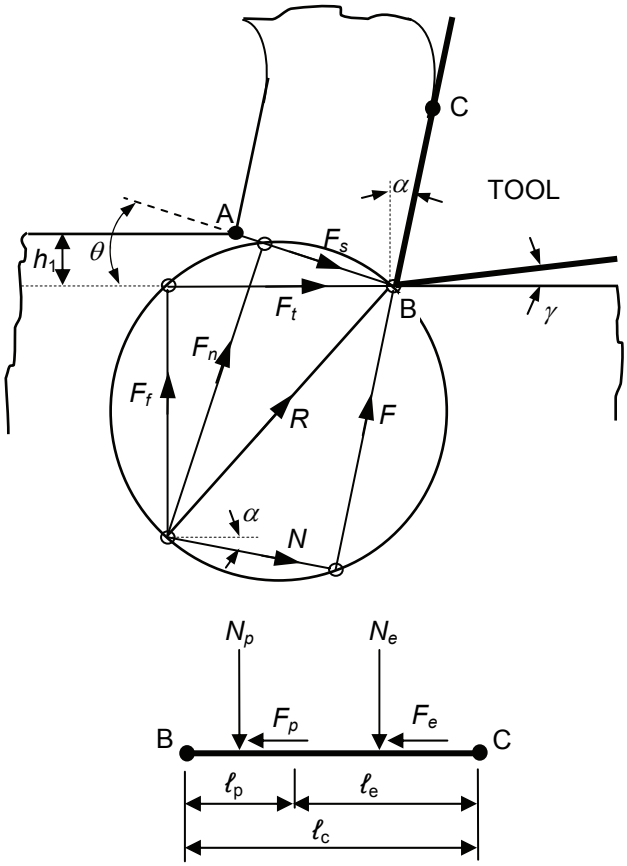

Figure 2: The Merchant's Circle and the schematic representation of the forces acting on the rake face.

P_0 in equation (3) which is needed to calculate most of the parameters can be obtained from the force equilibrium at the shear plane and the rake face as follows [22, 31]:

$$P_0 = \tau_1 \frac{h_1(\zeta + 1)}{\ell_c \sin\phi} \frac{\cos\lambda}{\cos(\phi + \lambda - \alpha)} \tag{6}$$

where h_1 is the uncut chip thickness, λ is the friction angle, and α is the rake angle. Also from the moment equilibrium at the tool tip the length of the contact and sticking region are obtained as follows [31]:

$$\ell_c = h_1 \frac{\zeta + 2}{2} \frac{\sin(\phi + \lambda - \alpha)}{\sin\phi \cos\lambda} \tag{7}$$

$$\ell_p = \ell_c \left(-\left(\frac{\tau_1}{P_0 \mu} \right)^{1/\zeta} + 1 \right) \quad (8)$$

Finally the apparent friction coefficient μ_a is calculated as follows [31]:

$$\mu_a = \frac{\tau_1}{P_0} \frac{\ell_p(\zeta + 1) + \ell_e}{\ell_c} \quad (9)$$

2.2 Solution Procedure

The model presented in the previous section can be used to predict the cutting forces provided that the friction coefficients and material model, i.e. the Johnson Cook parameters are known. The friction coefficient is determined from the orthogonal tube cutting tests by calculating the sliding friction coefficient iteratively. The number of tests is reduced compared with the conventional orthogonal tube cutting tests since the model can handle the effect of the rake angle. Therefore, it is sufficient to carry out tests for different cutting speeds and feed rates. The proposed solution procedure is as follows. Once the apparent friction is known all the unknowns up to Equation 8 can be calculated. The sliding friction coefficient is needed in order to calculate ℓ_p. An iterative search loop is used to calculate μ_a (Equation 9) by comparing with the measured μ_a values. Once the error between the calculated and measured μ_a is acceptable, the solution is found. Then, the tangential F_t and feed F_f cutting forces can be calculated using the following:

$$F_t = \tau_1 \frac{w h_1}{\sin\phi} \frac{\cos(\lambda - \alpha)}{\cos(\phi + \lambda - \alpha)}$$
$$F_f = \tau_1 \frac{w h_1}{\sin\phi} \frac{\sin(\lambda - \alpha)}{\cos(\phi + \lambda - \alpha)} \quad (10)$$

where w is the width of cut. In the proposed model, the shear angle is determined iteratively based on the minimum energy.

2.3 Identification of the friction coefficients

In this section experimental methods are described in order to identify the apparent friction coefficient between the tool and the workpiece material. But beforehand it should again be mentioned here that only the apparent friction coefficient is needed for cutting force predictions. In order to measure the apparent coefficient of friction on the rake face, orthogonal tube cutting tests were carried out on a conventional lathe. The test setup involves a dynamometer and a DAQ setup in order to collect the cutting force data. After each experiment the chip thickness is measured in order to identify the shear angle. The thickness is determined by direct micrometer measurements and by also weight measurements, and the average value is used. The tests were conducted at different cutting speeds and feed rates. The apparent friction coefficient on the rake face between the tool and the workpiece is calculated as follows:

$$\mu = \tan\left(rake + \tan^{-1}\left(F_f / F_t \right) \right) \quad (12)$$

where F_f and F_t are the measured feed and tangential forces, respectively.

3 RESULTS AND DISCUSSIONS

In this section the predictions of the dual-zone model is compared with the experimental results. Firstly, the shear angle predictions of the proposed model are compared. Afterwards the forces predictions are presented along with the experimental results. Finally, the effect of the Johnson-Cook constitutive model is discussed. TPGN type uncoated carbide inserts were used during orthogonal tube cutting tests. The rake angle was 5º. Two different steels were used as the workpiece material: AISI 1050 and AISI 4340. The tests were conducted for different cutting speeds and feed rates. The Johnson-Cook parameters for these two materials are given in Table 1. The discussion on the selection of these parameters is presented in Section 3.3.

Mat.	A(MPa)	B(MPa)	n	M	ν
1050	880	500	0.234	0.0134	1
4340	945	500	0.26	0.015	1

Table 1: Johnson Cook constitutive relationship parameters for the workpiece materials.

3.1 Shear Angle Predictions

As discussed earlier the shear angle is determined based on the minimum cutting power calculations. The shear angle is also experimentally identified from the tube cutting tests through chip thickness measurements [10]. In addition, the shear angle is also predicted by the Merchant law as follows [1]:

$$\phi = \left(\pi / 2 + \alpha - \lambda \right) / 2 \quad (13)$$

The friction angle λ in Equation 13 is substituted from the experimental values. These two predictions along with the experimental results are shown in Figure 3.a for the AISI 1050 steel and in Figure 3.b for the AISI 4340 steel.

As can be observed from Figure 3 the proposed model predictions are closer to the experimental values. This is most probably due to

the fact that the Merchant's model doesn't consider the effect of the strain, strain rate, and temperature on the material behavior. Also, the rake contact is simply represented by a sliding friction neglecting the effect of the plastic deformation on the rake face. The maximum difference between the proposed model predictions and the experimental results is around 10% for both materials, whereas it is around 20% for the Merchant' model.

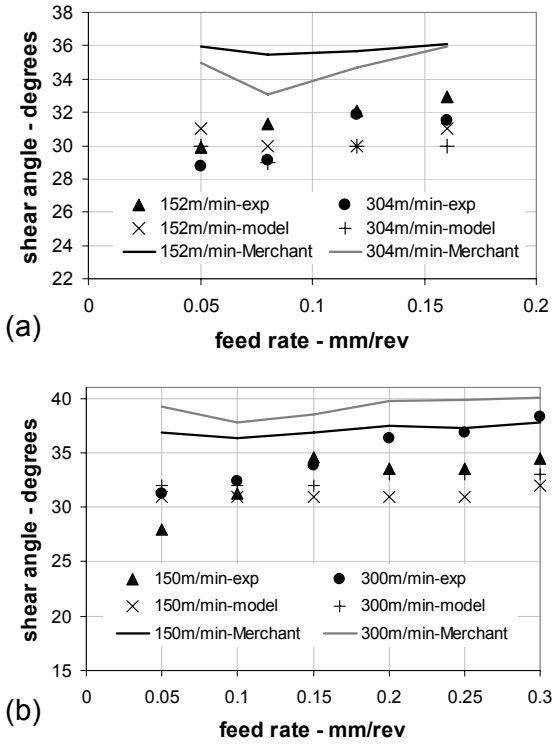

Figure 3: Comparison of shear angle predictions for (a) AISI 1050, and (b) AISI 4340 steels

3.2 Cutting Force Predictions

For a final verification, the cutting forces that are predicted by the proposed model are compared with the experimental results for various feed rates and cutting speeds. It should again be mentioned here that the apparent friction coefficients obtained from these tests are used in the force predictions. The results can be found in Figure 4 for the AISI 1050 steel and in Figure 5 for the AISI 4340 steel. As can be observed from the results, a strong agreement between the predictions and the experimental data is observed. The maximum and average discrepancies are 8% and 3%, respectively, which is mainly due to the inaccuracy in the material model. Although it is discussed in Section 3.3, it should be mentioned here again that the parameters of the material model are calibrated by only the shear stress obtained from the tube cutting tests. The apparent friction coefficients obtained from the experiments are also used in the force prediction. These inputs enable the proposed model to predict even small changes in the forces with the cutting speed and feed rate.

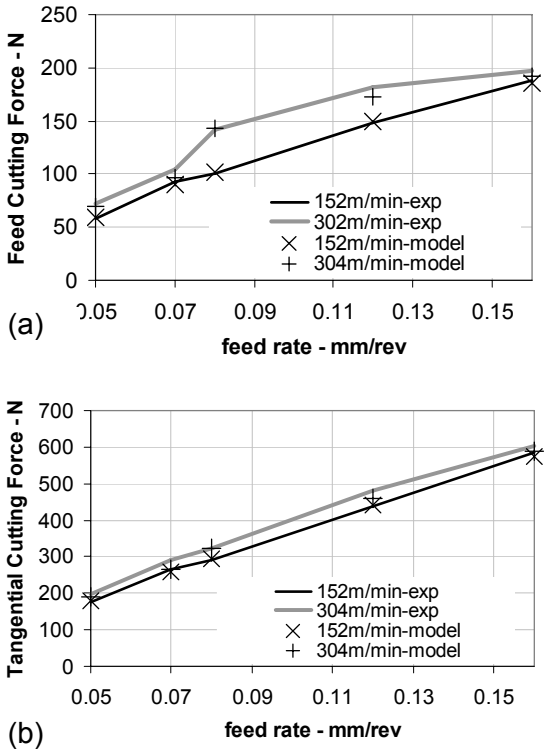

Figure 4: The (a) feed cutting force, and (b) tangential cutting force comparisons for the AISI 1050 steel.

3.3 Discussion on the constitutive model

As mentioned in Section 2.2 the only inputs required by the model are the material parameters and the friction coefficient. An approach to obtain the friction coefficient is proposed and verified by the experiments in aforementioned analysis. However, the selection of Johnson Cook parameters is another important issue in the analysis. A common method to obtain the material parameters is the Split-Hopkinson Pressure Bar (SHPB) test. However, the strain rates in metal cutting may reach the order of 105 s^{-1}, whereas they are usually restricted to 104 s^{-1} in SHPB tests [41], which may be an error source. In this section, the selection procedure and effects of the Johnson Cook parameters on the cutting forces for AISI 4340 steel will be given. The same strategy for the AISI 1050 steel is followed. Three different parameter sets found in the literature [42-44] for AISI 4340 steel are listed in Table 2.

Set	A(MPa)	B(MPa)	n	m	ν
2	792	510	0.26	0.014	1
3	950	725	0.375	0.015	0.625
4	910	586	0.26	0.014	1.03

Table 2: The JC parameters for 4340 steel obtained from three different studies [42-44].

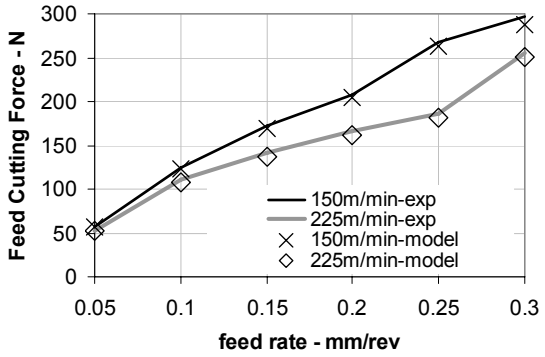

(a)

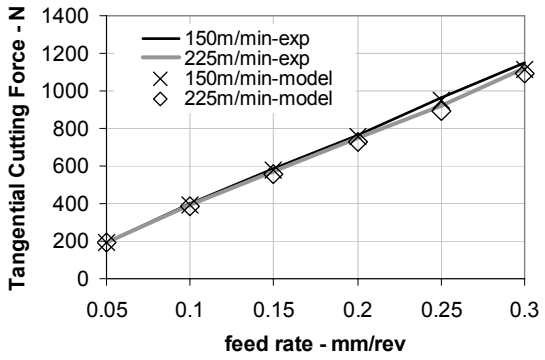

(b)

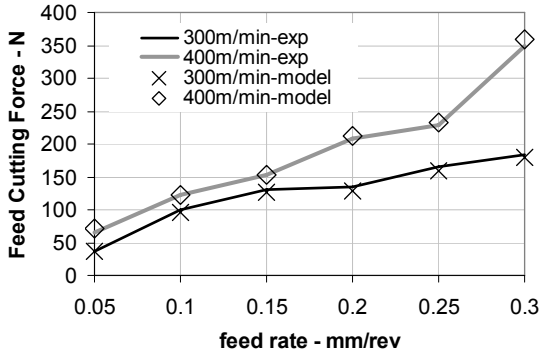

(c)

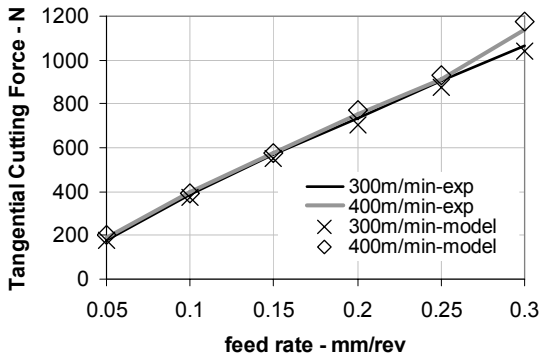

(d)

Figure 5: Feed cutting (a, c), and tangential cutting force (b, d) comparisons for AISI 4340.

In order to select the best parameter set we propose to apply a non-linear regression fitting procedure with the experimental data set using the shear stress at the shear plane. Due to the high sensitivity of the non-linear regression analysis to the initial and the tolerance values used, the number of parameters to be determined need to be reduced. If all the parameters of the Johnson Cook model are to be determined, the final values may turn out to be impractical. For instance, B can be found to be a negative number which is impossible. In order to solve this problem, we set the parameters B, n, m and ν as in Table 1, and solve for the parameter A which minimizes the error between the predicted and measured shear stresses. The results are shown in Table 1 which are called as set 1, and are used for all the predictions in Section 3. On the other hand, in order to compare the fitted parameters and the parameters that are found in the literature (see Table 2) a comparison for the cutting forces are conducted using these sets. The results can be found in Figure 6 for the tests conducted at 225 m/min cutting speed for different feed rate values.

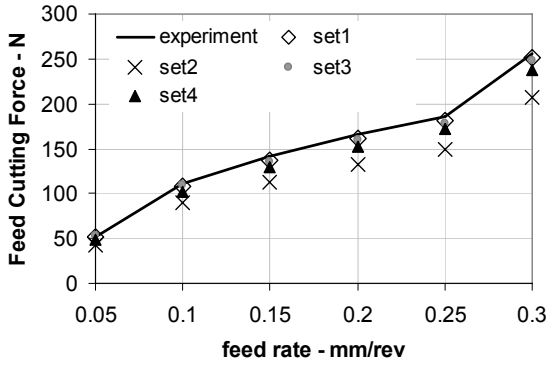

(a)

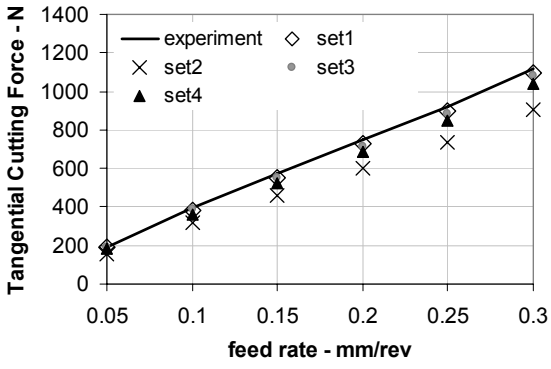

(b)

Figure 6: The (a) feed and (b) tangential cutting forces that are predicted by different set of Johnson Cook parameters.

As can be observed from Figure 6, Set 1, i.e. the material model obtained through non-linear regression analysis from the cutting test results, provide very good predictions. Set 3 also provide close predictions although they are quite different parameters. This is an important out-

come as it shows that different Johnson Cook parameter values may yield to the same results. Set 2, on the other hand, yields a higher error which shows that using preset values of Johnson-Cook model may sometimes yield inaccurate predictions. Thus, it is important to check the material parameters for different ranges of cutting conditions than the calibration range. Accurate results can be obtained by calibrating the material model using cutting data. The results presented in this section may also be an indication of the fact that the Johnson-Cook constitutive law may not be the best representation of the material behavior for metal cutting operations.

4 CONCLUSIONS

In this study an orthogonal cutting process model is proposed where the primary and secondary shear zones are modeled. A Johnson-Cook law is used to model the viscoplastic flow within the primary shear zone. A dual zone representation is used for the rake contact. The first region of the rake contact is modeled by sticking friction which is followed by a sliding friction zone. The mathematical formulation and solution procedure for the cutting forces are presented as well as the identification of the friction coefficients. It is proposed to obtain the apparent friction coefficient from orthogonal tube cutting tests and to calibrate the sliding friction coefficient by the proposed model. The results for shear stress and cutting forces are compared with the experimental values and good agreement is observed. Finally, the Johnson-Cook constitutive relationship parameter selections are discussed, and it is shown that different set of values may yield similar results due to the non-linear behavior of these equations.

5 ACKNOWLEDGMENTS

The orthogonal tube cutting tests for the AISI 4340 steel conducted by Mr. L. Taner Tunc and Mr. Burak Aksu are appreciated.

6 REFERENCES

[1] Merchant, E., 1945, Mechanics of the Metal Cutting Process I. Orthogonal Cutting and a Type 2 Chip, Journal of Applied Physics, 16/5:267-275.

[2] Cumming, J. D., Kobayashi, S., and Thomsen, E. G., 1965, "A New Analysis of the Forces in Orthogonal Metal Cutting," ASME J. Eng. Ind., 87:480–486.

[3] Zorev, N. N., 1963, Inter-relationship between shear processes occurring along tool face and shear plane in metal cutting, International Research in Production Engineering, ASME, New York, 42-49.

[4] E.H. Lee and B.W. Shaffer, 1951, The Theory of plasticity applied to a problem of machining, Trans. ASME, J. Appl. Mech., 18:405–413.

[5] M. C. Shaw, N.H. Cook, and I. Finnie, 1953, The Shear-Angle Relationship in Metal Cutting", Transaction ASME, 75:273-283.

[6] Palmer, W.B., Oxley, P.L.B., 1959, Mechanics of Orthogonal Machining, Proc. Instn. Mech. Engrs., 173/24:623-638.

[7] Childs, T., 1980, Elastic Effects in Metal Cutting, Int. J. Mech. Sci., 22:457-466.

[8] Armarego, E.J.A. and Whitfield, R.C. 1985, Computer based modeling of popular machining operations for force and power predictions. Annals of the CIRP, 34: 65-69.

[9] Budak, E., Altintas, Y. and Armarego, E.J.A., 1996, Prediction of milling force coefficients from orthogonal cutting data. Trans. ASME J. of Man. Sci. and Eng., 118:216-224.

[10] Altintas, Y., 2000, Manufacturing Automation, Cambridge University Press.

[11] Lin, Z.C., Pan, W.C., 1995, Lo, S.P., A study of orthogonal cutting with tool flank wear ans sticking behavior on the chip-tool interface, J. Mat. Proc. Tech., 52, 524-538.

[12] Lo, S.P., Lin, Y., 2002, An investigation of sticking behavior on the chip-tool interface using thermo-elastic-plastic finite element method, J Mat. Proc. Tech., 121:285-292.

[13] Yen, Y., Jain, A., Altan, T, 2004, A finite element analysis of orthogonal machining using different tool edge geometries, J. Mat. Proc. Tech., 146:72-81.

[14] Umbrello, D., Saoubi, R., Outeiro, J.C., 2007, The influence of Johnson–Cook material constants on finite element simulation of machining of AISI 316L steel, Int. J. Machine Tools&Manufacture, 27:462-470.

[15] Oxley, P.L.B., 1989, Mechanics of Machining, an Analytical Approach to Assessing Machinability, Ellis Horwood Limited, England.

[16] Fang, N, 2003, Slip-line modeling of machining with a rounded-edge tool – Part 1: new model and theory, J. Mechanics and Physics of Solids, 51:715-742.

[17] Fang, N., Jawahir, I.S., 2001, A new methodology for determining the stress state of the plastic region in machining with restricted contact tools, Int. J. Mech. Sci., 43: 1747-1770.

[18] Maity, K.P., Das, N.S., A Class of slipline field solutions for metal machining with sticking-slipping zone including elastic contact, Mater Design, doi:10.1016/j.matdes. 2006.07.014.
[19] Kudo, H., 1965, Some new slip-line solutions for two-dimensional steady-state machining, Int. J. Mech. Sci. 7:43-55.
[20] Yellowley, I., 1987 A Simple Predictive Model of Orthogonal Metal Cutting, Int. J. Mach. Tools Manufact., 27/3:357-365.
[21] Dudzinski, D., and Molinari, A., 1997, A Modelling Of Cutting For Viscoplastic Materials, Int. J. Mech. Sci, 39/4:369-389.
[22] Moufki, A., Molinari, A., and Dudzinski, D., 1998, Modelling of Orthogonal Cutting with a Temperature Dependent Friction Law, J. Mech. Phys. Solids, Vol. 46/10:2103-2138.
[23] Karpat, Y., Ozel, T., 2006, Predictive Analytical and thermal Modeling of Orthogonal Cutting Process – Part 1: Predictions of Tool Forces, Stresses, and Temperature Distributions, J. Manuf. Sci Eng., 128:435-444.
[24] Bailey, J.A., 1975, Friction in metal machining-mechanical aspects, Wear, 31: 243-275.
[25] Philippon, S., Sutter, G., Molinari, A., 2004 An experimental study of friction at high sliding velocities, Wear, 257:777-784.
[26] Tao, Z., Lovell, M.R., Yang, J.C., 2004, Evaluation of interfacial friction in material removal processes: the role of workpiece properties and contact geometry, Wear, 256:664-670.
[27] Fang, N., 2005, Tool-chip friction in machining with a large negative rake angle tool, Wear, 258:890-897.
[28] Childs, T.H.C., 2006, Friction modeling in metal cutting, Wear, 260:310-318.
[29] Ozel, T., 2006, The influence of friction models on finite element simulations of machining, Int. J. Machine Tools & Manufacture, 46:518-530.
[30] Kilic, D.S., Raman, S., 2006, Observations of the tool-chip boundary conditions in turning of aluminum alloys, Wear, doi:10.1016/j.wear.2006.08.019.
[31] Ozlu, E., Budak E., 2007, Experimental Analysis and Modeling of Orthogonal Cutting Using Material and Friction Models, Die and Mold Conference, Çeşme, Turkey.
[32] Filice, L., Micari, F., Rizutti, S., and Umbrello, D., 2007, A critical analysis on the friction modeling in orthogonal machining, Int. J. Mach. Tools&Manufacture, 47:709-714.
[33] Buryta, D., Sowerby, R., and Yellowley, I., 1994, Stress Distributions on the Rake Face During Orthogonal Machining, Int. J. Mach. Tools Manufact., 34/5:721-739.
[34] Arsecularatne, J. A., 1997, On Tool-Chip Interface Stress Distributions, Ploughing Force and Size Effect in Machining, Int. J. Mach. Tools Manufact., 37/7: 885-899.
[35] Rabinowicz, E., 1995, Friction and Wear of Materials: Second Edition, Wiley-Interscience, New York, 102.
[36] Olsson, M.,Soderberg, S., Jacobson, S., Hogmark, S., 1989, Simulaton of cutting tool wear by a modified pin-on-disc test, Int. J. Mach. Tools Manufact., 29/3:377-390.
[37] Kato, S., Yamaguchi, K., and Yamada, M., 1972, Stress Distribution at the Interface Between Tool and Chip in Machining, Journal of Eng. For Industry, 683-689.
[38] Barrow, G., Graham, T., Kurimoto, T., and Leong, F., 1982, Determination of Rake Face Stress Distribution in Orthogonal Machining, Int. J. Mach. Tool. Des. Res., 22/1: 75-85.
[39] Maclain, B., Batzer, S.A., and Maldonado, G. I., 2002, A numeric investigation of the rake face stress distribution in orthogonal machining, J. Materials Proc. Tech., 123: 114-119.
[40] Altan, T., Oh, S., Gegel , H.L., 1983, Metal forming : fundamentals and applications, Metals Park, OH : American Society for Metals.
[41] Meyers, M.A., 1994, Dynamic Behavior of Materials, John Wiley&Sons.
[42] Guo, Y.B. , Yen, D.W., 2004, A FEM Study on Mechanisms of Discontinuous Chip Formation in Hard Machining, J. Materials Processing Technology, 155-156:1350-1356.
[43] Ng, E.-G., Tahany I. E.W., Dumitrescu, M., and Elbastawi, M.A., 2002, “Physics-based simulation of high speed machining”, Machining Science and Technology, 6/3:301-329.
[44] Rattazi, D., J., 1996, Analysis of Adiabatic Shear Banding in aThick-Walled Steel Tube by the Finite Element Method, Ph.D. Thesis, Virginia Polytechnic Institute and State University